be steady and the thermocouples must be placed along an isotherm in the gas. The thermocouple junction must be at a location in the wire where the second derivative of temperature with respect to the axial coordinate of the thermocouple wire is negligible. No information about the radiative environment is required but the radiative and convective heat-transfer characteristics of the sensor must be known in the general case. Evaluation of a geometric shape-emissivity factor[2] is never required.

The principle of operation can be extended to any kind of temperature sensor if two geometrically similar sensors of slightly different sizes are available and if there is no conduction loss through the sensor supports.

References

[1] Rohsenow, W. M. and Choi, H., *Heat, Mass and Momentum Transfer*, Prentice-Hall, Englewood Cliffs, N.J., 1961, p. 200.

[2] Rohsenow, W. M. and Choi, H., *Heat, Mass and Momentum Transfer*, Prentice-Hall, Englewood Cliffs, N.J., 1961, p. 346.

Smooth Empirical Bayes Estimation of Observation Error Variances in Linear Systems

H. F. MARTZ JR.* AND M. W. LIAN†
Texas Tech University, Lubbock, Texas

Introduction

IN Ref. 1, an empirical Bayes estimator was developed for estimating the unknown random observation error variances in a discrete time linear system. There it was assumed that each unknown variance could be represented as the product of a known nominal value and an unknown random scale factor which is to be estimated.

A continuous empirical Bayes smoothing technique is developed in Ref. 2. This technique provides estimators possessing smaller average squared error losses than the type of empirical Bayes estimator employed in Ref. 1. A similar smooth empirical Bayes estimator was developed in Ref. 3, where a continuous prior density function approximation was "smoothed" through a suitable function of the observation data.

In this Note, a smooth empirical Bayes estimator is developed for estimating the unknown random scale component of each observation error variance. This estimator will be shown to possess a smaller average squared error loss than the estimator presented in Ref. 1.

Scale Factor Estimation

Consider the linear discrete dynamic system given by

$$x_i = \phi_i x_{i-1} + u_{i-1} \tag{1}$$

augmented by the linear observation—state equation

$$y_i = H_i x_i + v_i, \qquad i = 1,2,\ldots \tag{2}$$

with the same assumptions as in Ref. 1. As in Ref. 1 the observation error covariance matrix R_i is represented by the diagonal matrix

$$R_i = \text{diag}(r_{i1}^2/\theta_{i1}, r_{i2}^2/\theta_{i2}, \ldots, r_{iq}^2/\theta_{iq}) \tag{3}$$

where q is the number of observation types available, r_{ij}^2 is a known nominal value of the observation error variance associated with the jth observation type at time epoch i. Also, the scale factors $\{\theta_{ij}: i = 1,2,\ldots\}$ are independent realizations of a random variable Θ_j having a completely unknown and unspecified prior density function $g_j(\theta)$ which is zero on the negative real numbers and which may be different for each observation type.

From the usual Gaussian assumption on v_i in Eq. (2), it follows that

$$z_{ij} = (y_{ij} - h_{ij} x_i)/r_{ij}, \qquad i = 1,2,\ldots,n_j \tag{4}$$

conditional on θ_{ij}, is distributed with probability density function given by

$$f(z_{ij}|\theta_{ij}) = \theta_{ij}^{1/2}(2\pi)^{-1/2} \exp[-\theta_{ij} z_{ij}^2/2] \tag{5}$$

Here h_{ij} is the jth row of H_i and n_j is the total number of observations of type j available up to the present time. For simplicity, we let $n_j = n$ and shall drop the subscript j for the remainder of this section.

The Bayes estimator for θ_n is given by

$$E(\theta_n|z_n) = \int_0^\infty \theta_n f(z_n|\theta_n) g(\theta_n)\, d\theta_n \Big/ \int_0^\infty f(z_n|\theta_n) g(\theta_n)\, d\theta_n \tag{6}$$

According to a technique developed in Ref. 4 and used in Refs. 2 and 3, the prior density function $g(\theta_n)$ may be estimated by means of the approximation given by

$$g_n(\theta_n) = \frac{K}{nh(2\pi)^{1/2}} \sum_{i=1}^{n} \exp\left[-\frac{1}{2}\left(\frac{\theta_n - \hat{\theta}_i}{h}\right)^2\right], \quad 0 < \theta_n < \infty \tag{7}$$

where $h = h(n) = n^{-1/5}$, $\hat{\theta}_i$ is a suitably chosen estimate of θ_i to be discussed later, and where

$$K = \left[1 - \frac{1}{n}\sum_{i=1}^{n} \phi\left(\frac{-\hat{\theta}_i}{h}\right)\right]^{-1} \tag{8}$$

In Eq. (8), $\phi(\cdot)$ denotes the standard normal cumulative distribution function.

Inserting Eqs. (5) and (7) into Eq. (6), collecting terms, performing the indicated integrations, and simplifying, yields the smooth empirical Bayes estimator for θ_n given by

$$\tilde{\theta}_n = E_n(\theta_n|z_n) = \left(\frac{3}{2}h\right) \sum_{i=1}^{n} \exp[-a_i] U(2,b_i) \Big/ \sum_{i=1}^{n} \exp[-a_i] U(1,b_i) \tag{9}$$

where

$$a_i = (3z_n^4 h^4 + 8z_n^2 \hat{\theta}_i^2 h^2 + 4\hat{\theta}_i^2 - 4h^3 z_n^2 \hat{\theta}_i)/16h^2 \tag{10}$$

$$b_i = (z_n^2 h^2 - 2\hat{\theta}_i)/2h \tag{11}$$

and where $U(c,x)$ is the parabolic cylinder function[5,6] defined by

$$U(c,x) = [e^{-x^2/4}/\Gamma(c+1/2)] \int_0^\infty e^{-xy-y^2/2} y^{c-1/2}\, dy \tag{12}$$

Numerous asymptotic expansions exist for evaluating $U(c,x)$. In particular the form given in Ref. 5 in Sec. 19.12.3, in conjunction with the asymptotic expansion in Sec. 13.1.2, was used here for evaluating Eq. (12).

The entire preceding development was undertaken on the assumption that the true state vector x_n is known. Specifically x_n was used in obtaining z_n in Eq. (4). This is clearly not the case, and the estimate for x_n given by

$$\bar{x}_n = \phi_n \hat{x}_{n-1} \tag{13}$$

where $\hat{x}_{n-1}$ is the Kalman, Empirical Bayes filter estimate for x_{n-1} given in Ref. 1, is used.

Now consider the estimates $\hat{\theta}_i$ required in Eq. (9). The preceding estimates obtained from Eq. (9) for $i = 1,2,\ldots,n-1$, i.e. $\tilde{\theta}_1, \tilde{\theta}_2, \ldots, \tilde{\theta}_{n-1}$, can be substituted for $\hat{\theta}_1, \hat{\theta}_2, \ldots, \hat{\theta}_{n-1}$ respectively when calculating $\tilde{\theta}_n$. Also, the maximum likelihood estimate for θ_n given by $1/z_n^2$ may be substituted for $\hat{\theta}_n$ in Eq. (9) or a estimate of θ_n such as that provided by Ref. 1 could be employed. For simplicity the maximum likelihood estimate was used here.

Received January 6, 1972. This research was supported by NASA Grant NGR 44-011-040.

Index categories: Navigation, Control, and Guidance Theory; Spacecraft Tracking.

* Associate Professor of Industrial Engineering and Statistics.

† Research Assistant, Department of Industrial Engineering.

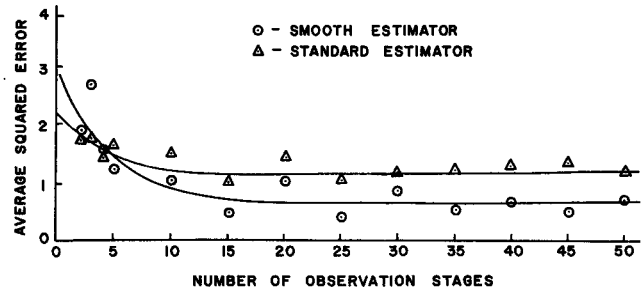

Fig. 1 Average squared error performance of the standard and smooth empirical Bayes estimators.

Performance Comparison

Monte Carlo simulation was employed to examine the average squared error loss incurred in using the estimator given by Eq. (9). For purposes of comparison the same dynamic system exemplified in Ref. 1 was again used here. The squared estimation errors $(\tilde{\theta}_n - \theta_n)^2$ were averaged for all five observation types over twenty-five replications for the standard estimator presented in Ref. 1 as well as for the estimator given here. The average squared errors are plotted in Fig. 1 at every fifth observation stage for both types of estimators. We observe that except for the first five stages, the smooth empirical Bayes estimator has an average squared error which is somewhat smaller than the standard empirical Bayes estimator. The same basic results were observed for numerous simulation runs using different sets of parameters. Thus, it appears that the estimator in Eq. (9) is somewhat superior in average squared error performance to the estimator in Ref. 1 and any gains should, in theory at least, be passed on to the Kalman state estimation procedure presented in Ref. 1.

References

[1] Martz, H. F. and Born, G. H., "Empirical Bayes Estimation of Observation Error Variances in Linear Systems," *AIAA Journal*, Vol. 9, No. 6, June 1971, pp. 1183–1187.

[2] Bennett, G. K. and Martz, H. F., "A Continuous Empirical Bayes Smoothing Technique," *Biometrika*, Vol. 59, No. 2, Aug. 1972, to be published.

[3] Martz, H. F. and Kamat, S. J., "Empirical Bayes State Estimation in Discrete Time Linear Systems," *AIAA Journal*, Vol. 9, No. 8, Aug. 1971, pp. 1654–1656.

[4] Parzen, E., "On Estimation of a Probability Density Function and Mode," *Annals of Mathematical Statistics*, Vol. 33, 1962, pp. 1065–1076.

[5] Abramowitz, M. and Stegun, I. A., *Handbook of Mathematical Functions*, National Burequ of Standards Applied Mathematics Series, 55, 1964.

[6] Gradshteyn, I. S. and Ryzhik, I. M., *Table of Integrals, Series, and Products*, Academic Press, New York, 1965.

Spreading of a Turbulent Disturbance

MICHAEL C. FISCHER*
NASA Langley Research Center, Hampton, Va.

Nomenclature

M = Mach number
x = distance along model wall, m
y = distance perpendicular to model surface, cm
z = coordinate in lateral direction, cm
δ = boundary layer thickness, cm
ϕ_{lateral} = disturbance lateral spreading angle, deg
ϕ_{spread} = disturbance total vertical spreading angle, deg
ϕ_{wall} = disturbance vertical spreading angle relative to wall, deg

Subscripts

e = boundary-layer edge conditions
0 = disturbance origin
tr = start of transition

Received January 17, 1972.

* Aerospace Engineer, Viscous Flows Section, Hypersonic Vehicles Division.

IN spite of the many experimental and theoretical studies dealing with the initial instabilities and subsequent transitional turbulent development of a boundary layer, very little is actually known about the initial disturbance growth behavior within the boundary layer. A recent paper[1] verified that the mean flow profiles in the outer portion of a hypersonic boundary layer ($M_e = 14$) are affected by transitional flow far upstream of the transition location indicated by wall heat-transfer measurements. Furthermore, an approximate spreading angle from the disturbance center (assumed to be near the critical layer) to the wall was shown to be shallow $\phi_{\text{wall}} \simeq 0.60°$. This Note extends the analysis of Ref. 1 to show the effect of local Mach number on both the turbulent disturbance spreading angle relative to the wall as well as lateral spreading.

To illustrate the effect of local Mach number on wall and lateral disturbance spreading angles, data from numerous investigations[1–21] were collected. With the exception of Ref. 1, and recent unpublished data obtained by the present author, all disturbance angles relative to the wall were determined from investigations where hot-wire contours[2,3] or hot-film surveys[4,7,13,20] of a "laminar" boundary layer were obtained. The spreading angle relative to the wall is herein defined as the angle formed by extending a straight line from the initial location where sizeable disturbances were first detected (known x and y values) in the laminar boundary layer down to the measured wall transition location. In our previous work (Ref. 1 and recent unpublished data) detailed spark schlierens showed protuberances at the outer edge of a laminar boundary layer far upstream of the wall transition location. The x location where these protuberances were first observed was taken as the initial disturbance origin, and a straight line from the critical layer height,[22] $y \simeq 0.90\,\delta$, extended down to the wall transition location was taken as the wall spreading angle.

Lateral disturbance spreading angles were obtained from investigations of: turbulent bursts,[5,16] reported observations of transverse contamination,[6,8] turbulent wedges formed behind isolated roughness specks,[10,18,21] and observed transitional oil flow[9,11,14,15,17] or other[19] visualization surface patterns both

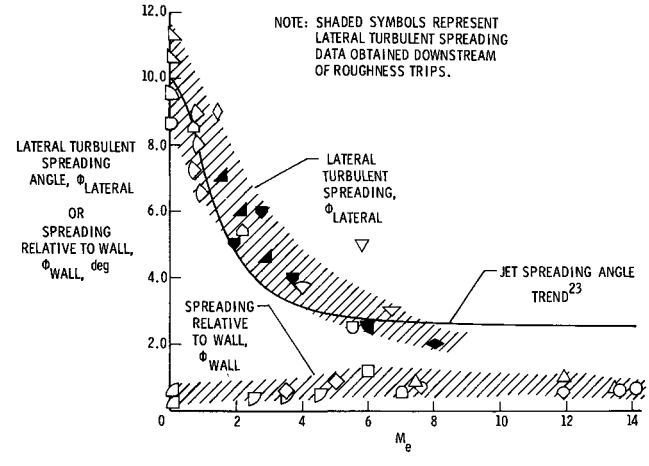

Fig. 1 Variation of turbulent spreading with local Mach number.